

See discussions, stats, and author profiles for this publication at: <https://www.researchgate.net/publication/231672499>

# Interlayer Structure of a Clay–Polymer–Salt–Water System

ARTICLE *in* LANGMUIR · JANUARY 2001

Impact Factor: 4.46 · DOI: 10.1021/la001353e

---

CITATIONS

30

---

READS

41

4 AUTHORS, INCLUDING:



[Jan Swenson](#)

Chalmers University of Technology

**177** PUBLICATIONS **3,998** CITATIONS

SEE PROFILE



[Mallika H L Bohm](#)

Tata Steel

**7** PUBLICATIONS **143** CITATIONS

SEE PROFILE



[Giovanna Fragneto](#)

Institut Laue-Langevin

**140** PUBLICATIONS **2,616** CITATIONS

SEE PROFILE

# Interlayer Structure of a Clay–Polymer–Salt–Water System

J. Swenson,<sup>\*,†</sup> M. V. Smalley,<sup>‡</sup> H. L. M. Hatharasinghe,<sup>‡</sup> and G. Fragneto<sup>§</sup>

*Department of Applied Physics, Chalmers University of Technology,  
S-412 96 Göteborg, Sweden, Department of Physics and Astronomy, University College  
London, London WC1E 6BT, United Kingdom, and Institut Laue-Langevin,  
BP 156, F-38042 Grenoble Cedex 9, France*

*Received September 21, 2000. In Final Form: January 11, 2001*

This paper presents a structural study of a four-component clay–polymer–salt–water system, consisting of *n*-butylammonium vermiculite, poly(ethylene oxide) (PEO), *n*-butylammonium chloride, and heavy water, using neutron diffraction and H/D isotope substitution of the butylammonium and PEO chains. The PEO molecules, salt ions, and water molecules are located in the interlayer regions between parallel and regularly spaced clay platelets. The results show that the added PEO does not cause any significant alteration in the distribution of butylammonium ions, when compared with the corresponding three-component system without added PEO. As in the three-component system, a major part of the butylammonium ions are located in a 4–5 Å thick layer at a distance of 12–16 Å from the center of the clay platelets. Rather than affecting the location of the butylammonium ions, some of the ethylene oxide segments partly displace water molecules immediately adjacent to the clay surfaces. Thus, the clay surfaces are covered by, first, one layer of adsorbed ethylene oxide segments and water molecules, second, another molecular layer of water, and, third, the layer of butylammonium ions. From the ordered structure around each clay platelet, we obtain a picture of an approximately 30 Å thick dressed macroion. The polymer segments that are not adsorbed onto the clay surfaces are rather homogeneously distributed in the interlayer region, at least in the present case with a high molecular weight PEO. Each polymer molecule adsorbs onto both clay surfaces and thereby induces a reduction of the interlayer spacing by a phenomenon known as polymer bridging flocculation.

## 1. Introduction

Clay systems are not only a central problem of geology and soil science; they are also remarkably useful as model systems in colloid, polymer, and biological sciences. Vermiculite clays consist of millions of negatively charged parallel silicate platelets that are held together by positively charged counterions located in the interlayer region. The usefulness of the clays as colloidal model materials lies in their ability to swell (up to 50 times) in the direction perpendicular to the silicate platelets by taking up water, salts, polymers, and other materials in the interlayer region.<sup>1</sup> The clay gel formed is an ideal one-dimensional colloidal system suitable for studies of electrostatic interactions and interlayer structure in colloidal suspensions and polyelectrolyte solutions.

The three-component system consisting of clay, salt, and water can be used to study the mechanism for charge stabilization of colloids,<sup>2</sup> and the corresponding four-component system with added polymer is an interesting model system for investigation of steric stabilization of colloids.<sup>3</sup> The latter is due to the adsorption of polymers onto the surface of colloidal particles, leading to a steric repulsion between them. Under certain circumstances, however, high molecular weight polymers can be adsorbed on separate particles and can draw them together, a phenomenon known as polymer bridging flocculation.<sup>4</sup>

This phenomenon has many important industrial applications in a large variety of areas, such as in the preparation of paints and papers, in the stabilization of drilling fluids, and in water purification,<sup>4</sup> where the flocs are used for the removal of unwanted particles.

In recent studies<sup>5,6</sup> we have elucidated the physical mechanism of polymer bridging flocculation, using small-angle scattering on a four-component clay–polymer–salt–water system, consisting of *n*-butylammonium vermiculite, poly(ethylene oxide) (PEO), *n*-butylammonium chloride, and heavy water.<sup>5,6</sup> We have also performed wide-angle neutron diffraction experiments on the same system, where we made use of the large difference in coherent scattering length between H and D ( $b_H = -3.74$  fm and  $b_D = 6.67$  fm) to determine the location of the ethylene oxide segments in the interlayer solution.<sup>7</sup> However, it is not only possible to perform H/D substitution of the polymer molecules; the same method can be used to determine the distribution of the butylammonium chains. Therefore, in this paper we have extended our previous diffraction study in ref 7 to include H/D substitution of both the polymer molecules and the butylammonium chains. We have also used an additional salt concentration in order to investigate the dependencies of the distributions of ethylene oxide segments and butylammonium chains on the concentration of *n*-butylammonium chloride in the interlayer solution.

<sup>†</sup> Chalmers University of Technology.

<sup>‡</sup> University College London.

<sup>§</sup> Institut Laue-Langevin.

(1) Walker, G. F. *Nature* **1960**, *187*, 312.

(2) See, for example: Smalley, M. V. *Langmuir* **1994**, *10*, 2884.

(3) Theng, B. K. G. *Formation and Properties of Clay-Polymer Complexes*; Elsevier: Amsterdam, 1979.

(4) Everett, D. H. *Basic Principles of Colloid Science*; Royal Society of Chemistry: London, 1988.

(5) Swenson, J.; Smalley, M. V.; Hatharasinghe, H. L. M. *Phys. Rev. Lett.* **1998**, *81*, 5840.

(6) Smalley, M. V.; Swenson, J.; Hatharasinghe, H. L. M.; Osborne, I.; Heenan, R. K.; King, S. M. *Langmuir*, submitted.

(7) Swenson, J.; Smalley, M. V.; Hatharasinghe, H. L. M. *J. Chem. Phys.* **1999**, *110*, 9750.

## 2. Experimental Section

The vermiculite crystals were from Eucatex, Brazil. Each crystal had an area of about 30 mm<sup>2</sup> and a thickness of approximately 1 mm, corresponding to a stack of almost 1 million parallel clay platelets. The crystals were washed and then treated for about 1 year with 1 M NaCl solution at 50 °C, with regular changes of solution, to produce a pure Na vermiculite, with the chemical formula<sup>8</sup> Si<sub>6.13</sub>Mg<sub>5.44</sub>Al<sub>1.65</sub>Fe<sub>0.50</sub>Ti<sub>0.13</sub>Ca<sub>0.13</sub>Cr<sub>0.01</sub>K<sub>0.01</sub>·O<sub>20</sub>(OH)<sub>4</sub>Na<sub>1.29</sub>. To prepare the *n*-butylammonium vermiculite, the Na form was soaked in 1 M *n*-butylammonium chloride solution at 50 °C, with regular changes of solution, for about 1 month. Chemical analysis of the *n*-butylammonium vermiculite thus obtained showed that the amount of interlayer sodium remaining was less than 1%. Crystals containing deuterated *n*-butylammonium ions were prepared from the protonated form by a further series of four exchanges carried out over a period of two weeks by soaking the crystals in a molar solution of the deuterated salt at 50 °C. The crystals were stored in a 1 M *n*-butylammonium chloride solution (of either H-salt or D-salt) prior to the swelling experiments.

The hydrogenous PEO was purchased from Scientific Polymer Products Ltd (Church Stretton, U.K.) with manufacturer's specifications  $M_w = 75\,000$  and  $M_w/M_n = 1.02$ , where  $M_w$  and  $M_n$  are the weight-average and number-average molecular weights, respectively, and used without further purification. The deuterated PEO was prepared from ethylene oxide-*d*<sub>4</sub> of 96% isotopic purity by Polymer Laboratories (Church Stretton, U.K.) with specifications  $M_w = 102\,000$  and  $M_w/M_n = 1.015$ . It should here be noted that the results obtained in ref 5 show that the difference in molecular weight between the hydrogenous and deuterated PEO has no effect on the *d*-spacing and probably only a minor influence on the distribution of the polymer segments located between the clay layers. The weak molecular weight dependence of the polymer distribution was further supported by the wide-angle diffraction study in ref 7. Thus, the difference in molecular weight between the hydrogenous and deuterated PEO should not affect the present analysis significantly. The solutions containing the volume fraction  $v = 0.04$  of hydrogenous and deuterated PEO were prepared by dissolving a known mass of the polymer ( $\rho = 1.13$  and  $1.23$  g/cm<sup>3</sup> for H-PEO and D-PEO, respectively) in a known volume of hydrogenous or deuterated *n*-butylammonium chloride solution, itself prepared by dissolving a known mass of *n*-butylammonium chloride in D<sub>2</sub>O. Thus, for each composition four samples (H-PEO and H-salt, D-PEO and H-salt, D-PEO and D-salt, and H-PEO and D-salt) were prepared. Furthermore, we prepared samples with two different concentrations of *n*-butylammonium chloride: 0.03 and 0.1 M. Because of the large incoherent scattering cross section of hydrogen, the crystals were swelled in D<sub>2</sub>O rather than H<sub>2</sub>O solutions. The gel samples were prepared at a sol concentration of  $r = 0.025$  by soaking a known mass of the vermiculite ( $\rho = 1.86$  g/cm<sup>3</sup>) in a known volume of the saline polymer solution. The swelling was carried out at  $T = 7$  °C in quartz jars for 2 weeks, to ensure that equilibrium had been achieved.<sup>9</sup>

Prior to the neutron diffraction experiments, the gel samples were removed from the soaking solution and cleaved, parallel to the silicate layers, using a razor blade. A sliver of the gel obtained was slid into a quartz cell of internal dimensions 20 mm high by 10 mm wide by 1 mm thick. The gels were placed in the sample can with the clay layers parallel to the 19 mm × 55 mm faces of the cell. To ensure that the sample remained in this orientation, individual gels were selected which were about 1 mm thick. Approximately half the amount of the soaking solution that had been in equilibrium with the gels was then added, giving a final volume fraction  $r$  of about 0.05. The presence of the solution was necessary to ensure that the gels remained in equilibrium but meant that there was a weak scattering contribution from fluid external to the gels. To ensure that the clays remained in the gel phase during the measurements, the samples were in thermal contact with a water bath at a temperature of 7 °C.

The neutron diffraction experiments were performed on the diffractometer D16 at the Institut Laue-Langevin (ILL), Grenoble,

France. The diffractometer has been described in detail elsewhere.<sup>10</sup> The samples were oriented such that the clay platelets were perpendicular to the momentum transfer vector  $Q$ , described as  $Q = Q_z$ . Spectra were recorded separately for each scattering angle, which was increased from 6° to 100° in steps of 2° (the detector covered about 9°), and also for monitors in the incident and transmitted beam. The incident wavelength was 4.53 Å. The data from the different scattering angles were then combined and corrected for background and container scattering and absorption. They were then normalized to a proper structure factor for the *z*-direction (perpendicularly to the clay platelets),  $S(Q_z)$ .

## 3. Results

Figures 1a–c and 2a–c show difference structure factors  $\Delta S(Q_z)$  (on different scales) of the four isotope compositions, H-PEO and H-salt, D-PEO and H-salt, D-PEO and D-salt, and H-PEO and D-salt, of 0.03 and 0.1 M butylammonium vermiculite gels, respectively. The difference structure factors  $\Delta S(Q_z)$  were obtained by subtraction of  $S(Q_z)$  of pure D<sub>2</sub>O from the measured  $S(Q_z)$ . In the lower  $Q$ -ranges shown in Figures 1a,b and 2a,b, we observe several orders of Bragg peaks due to interplatelet correlations, whereas Figures 1c and 2c show the diffuse scattering caused mainly by clay platelet–solution and solution–solution correlations in the higher  $Q$ -range. The correlations involving the solution may be due to an inhomogeneous distribution of polymer segments, butylammonium ions, and water molecules in the interlayer regions. From the positions of the Bragg peaks, it is clear that the *d*-spacing along the swelling axis was not identical for the four samples at each salt concentration, although they were prepared under the same  $r$ ,  $c$ ,  $v$  conditions. This is due to a combination of sample-to-sample variability, resulting from the fact that the original vermiculite crystals are from a naturally occurring clay mineral, and the difficulty in controlling the concentration variables when the gel slivers are loaded into the quartz cells.

From the positions of the Bragg peaks in Figures 1 and 2, it is clear that the *d*-spacing is approximately 90 Å for the 0.03 M salt concentration and about 60 Å in the case of the 0.1 M salt concentration. These values should be compared with the *d*-spacings of about 120 and 180 Å, respectively, for the corresponding three-component systems without added PEO. The strongly reduced *d*-spacing in the four-component system is due to a phenomenon known as polymer bridging flocculation.<sup>4</sup> The intensities of the first-order Bragg peaks are very different for the different isotope compositions because of the fact that the different isotope compositions give different scattering contrasts. The scattering contrast between the clay platelets and the interlayer solution will for instance increase if the polymer and butylammonium chains are protonated rather than deuterated. The intensities of the higher order Bragg peaks are particularly sensitive to the scattering density profile of the interlayer solution along the *z*-axis (perpendicular to the clay platelets). This means that a study of the intensities of higher order Bragg peaks of the different isotope compositions can provide information about the distributions of ethylene oxide segments and butylammonium chains in the interlayer solution. The same information, although on a more local length scale, is present in the diffuse scattering at higher  $Q$ -values. Thus, the interlayer structure can in principle be determined from a combined analysis of the diffuse scattering and the intensity variation (as a function of ordering) of the Bragg peaks of the four isotopically

(8) Jinnai, H.; Smalley, M. V.; Hashimoto, T.; Koizumi, S. *Langmuir* **1996**, *12*, 1199.

(9) Hatharasinghe, H. L. M.; Smalley, M. V.; Swenson, J.; Williams, G. D.; Heenan, R. K.; King, S. M. *J. Phys. Chem. B* **1998**, *102*, 6804.

(10) Samatey, F. A.; Zaccari, G.; Engelman, D. M.; Etchebest, C.; Popot, J. L. *J. Mol. Biol.* **1994**, *236*, 1093. <http://www.ill.fr/YellowBook/D16>.

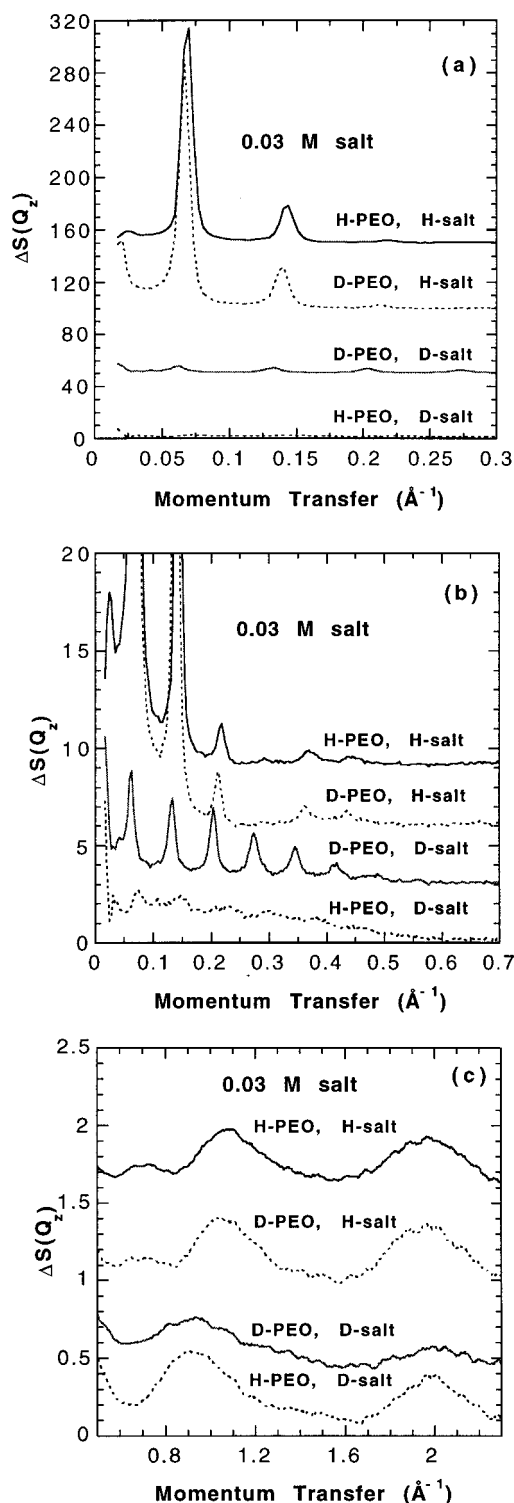


**Figure 1.** Difference structure factors  $\Delta S(Q_z)$  (obtained from the difference between the measured  $S(Q_z)$  of the samples and  $S(Q_z)$  of pure  $D_2O$ ) of the four isotopically different compositions, H-PEO and H-salt, D-PEO and H-salt, D-PEO and D-salt, and H-PEO and D-salt, with salt concentration  $c = 0.03$  M and volume fraction of PEO  $v = 0.04$ . The difference structure factors are shifted vertically and shown on three different scales in parts a–c, for clarity.

different samples. In practice, this is not an easy task, partly because of the sample-to-sample variability mentioned above but also because of the difficulty in extracting all the structural information that is present in the experimental data. To overcome this latter point, we have employed a modeling technique which is discussed below.

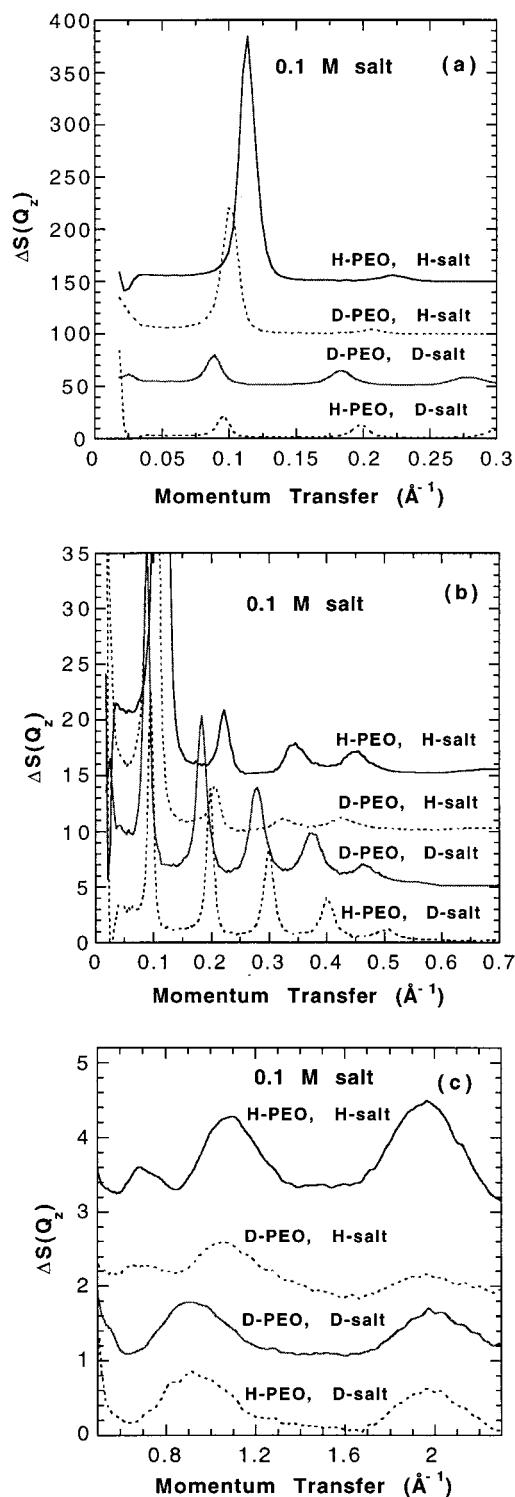


**Figure 2.** Difference structure factors  $\Delta S(Q_z)$  of the four isotopically different compositions, H-PEO and H-salt, D-PEO and H-salt, D-PEO and D-salt, and H-PEO and D-salt, with salt concentration  $c = 0.1$  M and volume fraction of PEO  $v = 0.04$ . The difference structure factors are shifted vertically and shown on three different scales in parts a–c, for clarity.

Before we move on to the structural modeling, we are, however, able to draw some conclusions directly from the experimental data. First, from a comparison of the data for the 0.03 and 0.1 M salt concentrations (see Figures 1 and 2) it is evident that the interlayer structure, that is, the distributions of the ethylene oxide segments and the butylammonium ions, must be very similar for the two salt concentrations, despite their different  $d$ -spacings. It



is also clear that H/D isotope substitution of the butylammonium chains has a much greater effect on the intensity of the Bragg peaks, as well as on the diffuse scattering pattern, than a corresponding substitution of ethylene oxide segments. This indicates that the butylammonium ions are much more inhomogeneously distributed in the interlayer solution, compared to the ethylene oxide segments.

To simplify the interpretation of the structural features observed in reciprocal space, each structure factor was Fourier transformed to a total neutron weighted one-dimensional pair correlation function along the  $z$ -axis:

$$G(r_z) = \frac{2 \sum_{i=1}^n c_i b_i^2}{\pi \rho_0 \left( \sum_{i=1}^N c_i b_i \right)^2} \int_0^\infty (S(Q_z) - 1) \sin(Q_z r_z) dQ_z + 1 \quad (1)$$

where  $\rho_0$  is the average number density and  $c_i$  and  $b_i$  are the concentration and neutron scattering length of atom  $i$ , respectively. However, the fact that the isotopically different samples have slightly different  $d$ -spacings complicates the analysis slightly. To make a proper structural comparison in real space of the isotopically different samples, we therefore had to scale their  $d$ -spacings to the same value before the Fourier transform was performed. Thus, the positions of the first- and higher order Bragg peaks had to be scaled to the same  $Q$ -values for all the four samples in order to remove differences in the diffraction data that are directly caused by their different  $d$ -spacings. The scaling was performed simply by compressing or expanding  $S(Q_z)$  of the four samples up to the  $Q$ -value of the position of the highest order Bragg peak, that is,  $Q \approx 0.5 \text{ \AA}^{-1}$ , to get the positions of the Bragg peaks to coincide for the samples. Further, we made the assumption that the different  $d$ -spacings affect only the positions of the Bragg peaks and that the length scale of all the other short and intermediate range correlations were the same for the four isotopically different samples. Thus, in order not to affect the diffuse scattering in the high  $Q$ -range we had to compensate the scaling of the positions of the Bragg peaks by an equal expansion or compression of the  $Q$ -range "between" the Bragg peaks and the diffuse scattering. This scaling procedure is of course by no means ideal because of the assumptions made and the fact that the positions of the higher order Bragg peaks are not well separated in  $Q$  from the diffuse scattering. However, the scaling of the  $d$ -spacing was necessary to obtain difference pair correlation functions  $\Delta G(r_z)$ , by subtracting one pair correlation function  $G(r_z)$  from another, without spurious peaks being introduced by the different  $d$ -spacings.

Figure 3 shows the difference function  $\Delta G(r_z) = G_D(r_z) - G_H(r_z)$  between the  $G(r_z)$  values obtained for the samples with deuterated and hydrogenous PEO, respectively. In the case of the 0.1 M salt concentration, the butylammonium chains were deuterated in both samples, whereas the counterions were hydrogenous in the two samples of 0.03 M salt concentration. Thus,  $\Delta G(r_z)$  should give us the correlations due to the replacement of hydrogenous PEO by deuterated PEO, which means that the correlations involving PEO should give positive contributions. Moreover, because we are using normalized  $G(r_z)$  (see eq 1) it is obvious that all the remaining correlations involving the clay layers,  $D_2O$ , and the butylammonium ions are less weighted for the deuterated sample and thus give

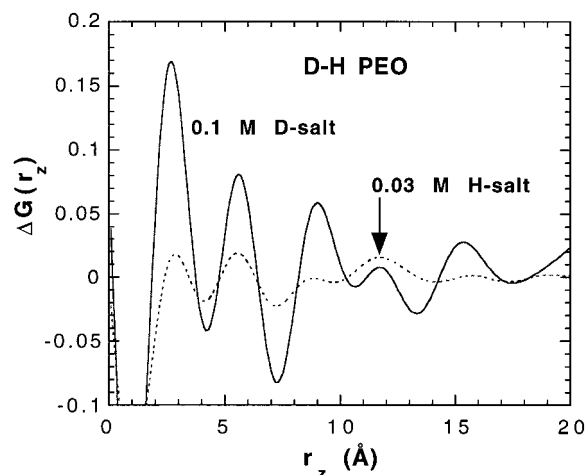


**Figure 3.** Difference pair correlation functions,  $\Delta G(r_z)$ , between the atomic pair correlation functions of samples with deuterated and hydrogenous PEO. In the case of the 0.1 M salt concentration (solid line), the butylammonium chains were deuterated in both samples, whereas for the 0.03 M salt concentration (dashed line) both samples contained hydrogenous counterions. The volume fraction of PEO was 4% in all cases.

negative contributions to  $\Delta G(r_z)$ . It can be seen in Figure 3 that for both salt concentrations  $\Delta G(r_z)$  shows five relatively sharp peaks located at approximately 3, 5.5, 9, 11.5, and 15 Å. The present result for the 0.1 M salt concentration is very similar to the previous finding presented in ref 7, although the real-space resolution of the data is lower in this case because of the limited  $Q$ -range. It is not worthwhile to repeat the same analysis here or discuss the results in detail. Instead, we will simply confirm our interpretation for the 0.1 M salt concentration and use Figure 3 to show that there is no indication that the distribution of ethylene oxide segments is significantly different for the 0.03 M salt concentration. Thus, we conclude that for both salt concentrations the results are consistent with the finding in ref 7 that some of the ethylene oxide segments are directly adsorbed on the clay surfaces. The majority of the ethylene oxide segments are, however, distributed in a Gaussian-like coil in the middle between the clay layers.<sup>7</sup> For the high molecular weight PEO studied, this means that after the polymer chains have induced a contraction of the interlayer spacing the polymer segments will be rather uniformly distributed in the interlayer region and therefore will not give rise to any strong features in the diffraction patterns, in agreement with the experimental findings. Therefore, some of the ethylene oxide segments displace water molecules immediately adjacent to the clay surfaces, bonding directly to them by physical adsorption, and the remaining polymer segments are rather uniformly distributed in the interlayer region. The reason for the fact that ethylene oxide segments adsorb on the clay surfaces is likely that the ether oxygens (Lewis bases) of PEO have a great affinity for the strong Brønsted acid sites on the silica-containing clay platelets. Similar findings have previously been observed for PEO in several aqueous and nonaqueous mediums, where it was shown that the oxygens of the ethylene oxide segments adhere strongly to  $SiO_2$  glass.<sup>11–14</sup>

(11) Mathur, S.; Moudgil, B. M. *J. Colloid Interface Sci.* **1997**, *196*, 92.

(12) Killmann, E.; Adolph, H. *Colloid Polym. Sci.* **1995**, *273*, 1071.

(13) Fytas, G.; Anastasiadis, S. H.; Seghouchi, R.; Vlassopoulos, D.; Li, J. B.; Theobald, W.; Toprakcioglu, C. *Science* **1996**, *274*, 241.

(14) Zheltonozhskaya, T. B.; Rudnitskaya, V. Z.; Eremenko, B. V.; Syromyatnikov, V. G. *Colloid J.* **1996**, *58*, 319.

It is interesting to know that the distribution of the ethylene oxide segments is rather independent of the salt concentration, but it was more important to investigate how the presence of the polymer affects the distribution of the counterions. To elucidate this in more detail, we have employed a modeling technique. This method is based on an inverse Monte Carlo based program, which simulates the scattering density profile along the  $z$ -axis (perpendicular to the clay platelets),  $\rho(z)$ , simultaneously for several isotopically different samples.<sup>15</sup> The method therefore enables us to use all the structural information present in the diffraction data simultaneously for two or more isotopically different samples. The resulting  $\rho(z)$  is the density profile which is in best agreement with the diffraction data. If we use two data sets, one in which the counterions are hydrogenous and one in which they are deuterated, two different density profiles are obtained: one for the counterions (because of the different scattering contrasts of the two data sets) and one for the remaining interlayer solution and the clay platelets. The neutron structure factor  $S(Q_z)$  is related to the neutron scattering density profile  $\rho(z)$  via the crystallographic structure factor,  $F(Q_z)$ , according to eqs 2 and 3:

$$S(Q_z) = M(Q_z) F(Q_z) F^*(Q_z) \quad (2)$$

$$F(Q_z) = \int_0^c \rho(z) [\cos(Q_z z) + i \sin(Q_z z)] dz \quad (3)$$

where  $c$  is the spacing between the clay layers ( $d$ -spacing) and  $M(Q_z)$  is a Lorentzian that takes into account the mosaic spread of the sample. Thus, this essentially crystallographic description is a method to produce a single particle distribution function,  $\rho(z)$ , rather than a spatially averaged pair correlation function,  $G(r_z)$ .

The crystallographic method cannot be very successfully used to determine the distribution of the ethylene oxide segments, because the differences in the diffraction data resulting from the sample-to-sample variability are of the same order as the differences induced by the replacement of hydrogenous PEO by deuterated PEO. However, H/D substitution of the butylammonium chains causes considerable alterations in the diffraction data, both in the intensity of the Bragg peaks and in the  $Q$ -range of the diffuse scattering (see Figures 1 and 2). Thus, the modeled scattering length density profile along the  $z$ -axis,  $\rho(z)$ , for the butylammonium chains, shown in Figure 4, should be at least qualitatively correct. Figure 4a shows  $\rho(z)$  for the composition with a salt concentration of 0.03 M, and the corresponding function for the 0.1 M salt concentration is shown in Figure 4b. The centers of the clay platelets are located at 0 and 90 Å in Figure 4a and at 0 and 62 Å in Figure 4b. By comparison of the two figures, it is evident that the distribution of butylammonium chains is qualitatively the same for the two salt concentrations. A particularly important result is that for both salt concentrations a major part of the butylammonium chains are located in a 4–5 Å thick layer at a distance of 12–16 Å from the center of the clay platelets; that is, they are situated just outside the approximately 6 Å thick layer of adsorbed polymer segments and water molecules. This means that the highest concentration of butylammonium chains is located at the same distance from the clay surfaces as in the corresponding three-component systems without added PEO.<sup>16,17</sup> Thus, there is no indication that

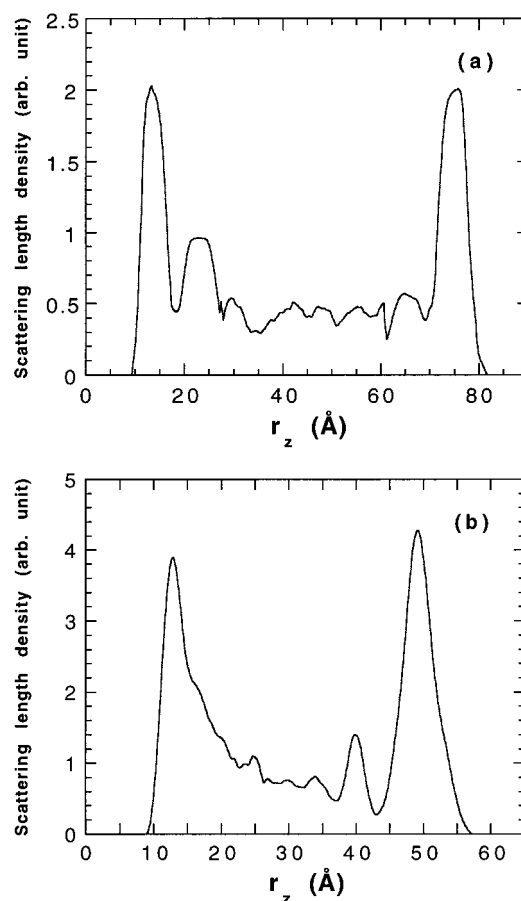


**Figure 4.** Scattering length density profiles along the  $z$ -axis,  $\rho(z)$ , of butylammonium chains in the interlayer region as a function of  $r_z$ . The salt concentration is 0.03 M in (a) and 0.1 M in (b), and the polymer volume fraction is 4% in both cases. The centers of the clay platelets are located at  $r_z = 0$  and  $r_z = 90$  Å in (a) and at  $r_z = 0$  and  $r_z = 62$  Å in (b). The results were obtained from structural modeling (see text) of the diffraction data shown in Figures 1 and 2.

the presence of PEO affects the distribution of the butylammonium ions.

#### 4. Discussion

Previous comprehensive neutron diffraction studies of the corresponding three-component system have both elucidated the interlayer structure<sup>16,17</sup> and determined how the  $d$ -spacing depends on hydrostatic pressure<sup>18</sup>  $P$ , temperature<sup>19</sup>  $T$ , uniaxial pressure along the swelling axis<sup>20</sup>  $p$ , the volume fraction of the clay in the condensed matter system (sol concentration)<sup>21</sup>  $r$ , and the electrolyte concentration in the aqueous solution<sup>1,2,18–21</sup>  $c$ . It is evident from the results that the  $d$ -spacing is very sensitive to all these parameters, whereas the structurally ordered interlayer range of about 10 Å on each side of the clay platelets is basically independent of the swelling conditions. These studies give rise to a consistent picture of a

(15) Williams, G. D.; Soper, A. K.; Skipper, N. T.; Smalley, M. V. *J. Phys. Chem. B* **1998**, *102*, 8945.

(16) Swenson, J.; Smalley, M. V.; Thomas, R. K.; Crawford, R. J.; Braganza, L. F. *Langmuir* **1997**, *13*, 6654.

(17) Swenson, J.; Smalley, M. V.; Thomas, R. K.; Crawford, R. J. *J. Phys. Chem. B* **1998**, *102*, 5823.

(18) Smalley, M. V.; Thomas, R. K.; Braganza, L. F.; Matsuo, T. *Clays Clay Miner.* **1989**, *37*, 474.

(19) Braganza, L. F.; Crawford, R. J.; Smalley, M. V.; Thomas, R. K. *Clays Clay Miner.* **1990**, *38*, 90.

(20) Crawford, R. J.; Smalley, M. V.; Thomas, R. K. *Adv. Colloid Interface Sci.* **1991**, *34*, 537.

(21) Williams, G. D.; Moody, K. R.; Smalley, M. V.; King, S. M. *Clays Clay Miner.* **1994**, *42*, 614.

30 Å thick dressed macroion composed of a clay platelet with exactly two layers of water molecules and one layer of counterions adsorbed onto each surface.<sup>16</sup> The well-defined nature of this structural unit and its persistence over such a wide range of thermodynamic conditions are obvious challenges to theory, because any continuum electrical theory, such as Derjaguin–Landau–Verwey–Overbeek theory<sup>22,23</sup> or Sogami theory,<sup>24,25</sup> predicts that a large fraction of the positively charged counterions should be directly adsorbed onto the negatively charged clay platelets. The reason for the contradictory finding in our studies may be the strong tendency of the counterions, and probably also the clay surfaces, to form hydration shells. Thus, the hydration forces seem to be stronger than the Coulomb interactions. In fact, a dressed macroion structure similar to what we have observed has been obtained from a theoretical one-dimensional adsorption model that includes nearest-neighbor electrostatic interactions for the competition between water and counterions for the adsorption sites at the clay surfaces.<sup>26</sup>

The interlayer structure and *d*-spacing of the corresponding four-component system is much less systematically investigated, although some interesting results have appeared.<sup>5–9</sup> For instance, high molecular weight polymers can induce a dramatic contraction of the interlayer spacing by bridging between two consecutive clay platelets and drawing them together by a phenomenon known as polymer bridging flocculation.<sup>4</sup> The simplicity of the present one-dimensional colloidal model system has enabled us to determine the strength and physical mechanism of this bridging phenomenon.<sup>5–7</sup> However, it has not been clear how the introduced polymer molecules affect the interlayer structure of the salt–water solution. This matter has been clarified in the present neutron diffraction study, where no evidence can be found that PEO alters the interlayer structure other than that some of the polymer segments displace water molecules immediately adjacent to the clay surfaces, bonding directly to them by physical adsorption. Thus, the very inhomogeneous distribution of the counterions remains basically unaffected and the structurally ordered range around each clay platelet is preserved, except for some directly adsorbed water molecules that have been displaced by ethylene oxide segments. At first sight, this seems to be a rather surprising result. The substantial rearrangement of the first layer of adsorbed water molecules necessary to accommodate the polymer segments may be expected to have a noticeable effect on both the adjacent layer of water molecules and their neighboring counterions. The appar-

ent insensitivity of the counterion layer 12–15 Å from the center of the clay platelets to the PEO adsorption 6–9 Å from the center of the clay platelets is also certainly due to the insensitivity of the dressed macroion structure to the thermodynamic conditions in the three-component system and raises another challenge to theory.

## 5. Conclusion

In previous neutron diffraction studies of the three-component system consisting of *n*-butylammonium vermiculite, *n*-butylammonium chloride, and heavy water, we were able to show that the clay surfaces are covered by two layers of water molecules, with the counterions at least 11 Å from the center of the clay layers.<sup>16,17</sup> In an earlier wide-angle study of the present four-component system, we showed that the structure of the dressed macroion (the charged clay particle with its associated layers of water molecules and counterions) is disrupted by the addition of PEO, with the ethylene oxide segments displacing water molecules immediately adjacent to the clay surfaces.<sup>7</sup> This latter result is confirmed in the present study, which furthermore enables us to draw the following conclusions:

(a) The earlier finding that ethylene oxide segments displace water molecules immediately adjacent to the clay surfaces seems to be a general result independent of the salt concentration, as long as the molecular weight of the polymer is high enough to permit the polymer to bridge between two consecutive clay platelets.

(b) The nonadsorbed polymer segments of high molecular weight PEO ( $M_w > 70\,000$ ) are rather uniformly distributed in the interlayer region.

(c) There is no indication that the presence of PEO affects the distribution of butylammonium ions. A major part of the butylammonium chains are located in a 4–5 Å thick layer situated just outside the approximately 6 Å thick layer of adsorbed polymer segments and water molecules.

(d) From the ordered interlayer structure (which seems to be independent of the salt concentration) around the approximately 10 Å thick clay platelet, we obtain a picture of a roughly 30 Å thick dressed macroion, including the clay platelet itself plus adsorbed layers of polymer segments, water molecules, and counterions.

**Acknowledgment.** We are grateful to Professor R. K. Thomas for providing us with the deuterated polymer. We thank Professors K. S. Schmitz and J. C. Selser for valuable discussions. This work was financially supported by Unilever PLC. H.L.M.H. thanks Unilever PLC for a studentship in support of the work, and J.S. thanks the Swedish Natural Science Research Council for their support.

LA001353E

(22) Derjaguin, B. V.; Landau, L. *Acta Physicochem.* **1941**, *14*, 633.

(23) Verwey, E. J. W.; Overbeek, J. Th. G. *Theory of the Stability of Lyophobic Colloids*; Elsevier: Amsterdam, 1948.

(24) Sogami, I. *Phys. Lett A* **1983**, *96*, 199.

(25) Sogami, I.; Ise, N. *J. Chem. Phys.* **1984**, *81*, 6320.

(26) Schmitz, K. S. *J. Phys. Chem. B* **1999**, *103*, 8882.